TUDelft

Delft University of Technology

Compensation Network for a 7.7 kW Wireless Charging System that Uses Standardized Coils

Grazian, Francesca; Shi, Wenli; Soeiro, Thiago B.; Dong, Jianning; van Duijsen, Peter; Bauer, Pavol

Important note
To cite this publication, please use the final published version (if applicable).
Please check the document version above.

Compensation Network for a 7.7 kW Wireless Charging System that uses Standardized Coils

Francesca Grazian, Wenli Shi, Thiago B. Soeiro, Jianning Dong, Peter van Duijsen and Pavol Bauer
Delft University of Technology
Delft, The Netherlands
Email: (F.Grazian, W.Shi-3, T.BatistaSoeiro, J.Dong-4, P.J.vanDuijsen, P.Bauer)@tudelft.nl

Abstract—**Industrial wireless charging systems use standardized coils to guarantee interoperability between different manufacturers. In combination with these coils, the compensation network can still be designed and optimized. This paper explains the step-by-step design of the compensation network for a 7.7 kW wireless charging system (power class WPT2), which is composed of standardized coils. The compensation network must satisfy the output power and voltage requirements, the soft-switching of the inverter, and the limit of voltage and current stress on the components. The S-S compensation network is found to be unfeasible for those coils, and an optimized double-sided LCC compensation network is designed. The 3-phase grid connection is selected despite the 1-phase one because it gives the lowest total conduction losses. Finally, two parallel SiC MOSFETs C3M0075120K are chosen as inverter's switch because of their low conduction losses. This solution can achieve a payback time within a year with respect to the cheapest one.**

Index Terms—**Compensation networks, electric vehicles (EVs), inductive power transfer, standardized coils, wireless charging.**

I. INTRODUCTION

Nowadays, standards and regulations on wireless charging for electric vehicles (EVs) are well defined, such that interoperability is guaranteed between systems from different manufacturers [1]. Especially for what concerns the main magnetic coils, reference designs are specified in SAE 2954 [2] for the power levels up to 11.1 kW (WPT3). Each of them presents both mechanical and electrical specifications. This means that the specification already defines the values of the inductance and coupling of the coils. From an industrial point of view, manufacturers commercialize coils which are designed based on the reference designs to make sure that their products are compatible with the standards.

When designing a wireless charging system using standardized coils, the compensation network can be still optimized. The aim of the compensation network is to minimize the reactive power circulating in the charging system. In this way, it is possible to transfer the required power to charge the battery and achieve high power efficiency. At the required power level, the compensation network must also ensures that the DC output voltage is in the range of the battery voltage, which is typically around 400V. At the same time, the DC input voltage must be in the range of the rectified voltage from the AC grid, which is either 340-500V DC in case of a 1-phase connection or 650-870V DC in case of a 3-phase one, for a grid with phase-to-neutral potential of 230 V rms. Moreover, the inverter's soft-switching needs to be guaranteed,

and the voltage and current stress on all components must be within reasonable values. Therefore, given the geometry and the electrical specifications of the coils, the designed compensation network needs to satisfy all these requirements.

This paper explains the design and the optimization of the compensation network for a 7.7 kW wireless charging system, which is composed of standardized coils of the power class WPT2. The coils parameters and the design constraints are summarized in Section II. After this, Section III explains the step-by-step design and optimization of the compensation network. Then, the stress on the components is computed through an accurate circuital model and time-domain simulations. The well-known series-series (S-S) compensation network is proved to be unfeasible with selected standardized coils for the required power level, and the double-sided LCC compensation network is found to be suitable. Different designs are analyzed and compared for what concerns the soft-switching of the inverter, the voltage and current stress, conduction losses of the components and cost. Finally, in Section IV, conclusions are given on the design of a 7.7 kW compensation network.

II. DESIGN REQUIREMENTS AND CONSTRAINTS

The compensation network has to be designed and optimized for a 7.7 kW wireless charging system with given coils. The equivalent circuit of the system is shown in Fig. 1. Standardized coils are used according to the power class WPT2 of SAE J2954 [2]. In particular:

– *Transmitter:* the coil is sealed in a concrete block to facilitate its on-ground mounting. Its geometrical and electrical characteristics are based on the universal ground assembly (GA) coil. This coil has been manufactured by MAGMENT [3].

– *Receiver:* the coil is based on the geometrical and electrical characteristics of the WTP2/Z2 class. This coil has been manufactured by PREMO [4].

Fig. 2 shows the picture of the two coils of the wireless charging system. The coils' parameters are constraints in the design of the whole wireless charging system. In particular, L_1 and L_2 define the transmitter (primary) and receiver (secondary) coil inductance; R_1 and R_2 are, respectively, their series resistances; M is the mutual inductance between the coils, and k is their coupling factor ($k = \frac{M}{\sqrt{L_1 L_2}}$).

For what concerns the requirements, the output power P_{out} is defined by the receiver's coil power class. The DC output
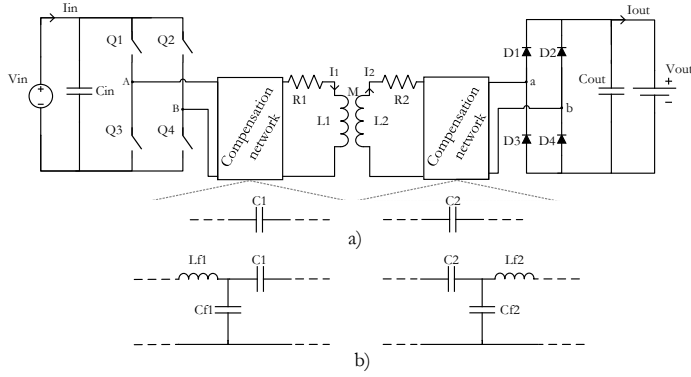
Fig. 1. Equivalent circuit of a 7.7 kW wireless charging system, using as compensation network: a) S-S, b) double-sided LCC.
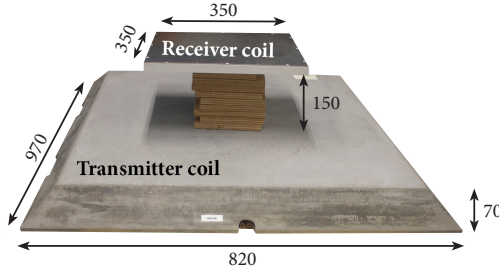

Fig. 2. Aligned transmitter and receiver coils. Dimensions are in mm.

voltage V_{out} is considered to be equal to the nominal voltage of a conventional battery used in automotive applications. The DC input voltage V_{in} must be within the grid's rectified voltage range. The nominal operating frequency f_0 and its allowed range are defined in [2]. Another essential requirement is to have reasonable voltage and current stresses $\hat{V}$, $\hat{I}$ on the components, such that they do not exceed their capability and, at the same time, they guarantee proper operation and high efficiency of the power electronics. Finally, the compensation network needs to ensure the soft-switching of the inverter.

All these parameters of the constraints and requirements are summarized in Table I. The values regarding the coils are measured at the specified airgap and with perfect alignment.

III. DESIGN PROCEDURE

It is always preferable to choose a compensation network with the minimum number of components, such that the losses can be contained. From the literature, it is well-known that at least one capacitor must be connected to each coil. In this way, the reactive power that circulates in the system is minimized, and the power factor is closed to unity at both the input and output of the resonant stage. Depending on the type of connection, the most basic compensation network can be either series-series (S-S), series-parallel (S-P), parallel-series (P-S) or parallel-parallel (P-P) [5]–[10]. Among these combinations, the S-S compensation is the most used in wireless charging because the required value of both capacitors is independent of both coupling and loading condition [5], [9]–[11]. Its schematic is shown in Fig. 1a).

Compensation networks with multiple components can be also found in the literature, such as the double-sided LCC compensation network which the schematic is shown in Fig.

TABLE I
DESIGN CONSTRAINTS AND REQUIREMENTS.

Requirements	P_{out}	7.7 kW	**Constraints**	L_1	63.35 µH
	V_{out}	400 V		L_2	43.53 µH
	V_{in}	340-500 V (1ϕ) or		R_1	187 mΩ
		650-870 V (3ϕ)		R_2	62 mΩ
	f_0	85 kHz (79-90 kHz)		M	7.4 µH
	$\hat{V}$, $\hat{I}$	< 5 kV, 80 A		k	0.14
	Q1...Q4	Soft-switching		airgap	150 mm

1b) [12]–[16]. According to [12], this network has several features. First, the current flowing through the primary coil does not depend neither on the coupling nor on the load condition. This property is preferable both in dynamic charging and when multiple receivers are present. After this, since the resonant voltage is shared by more components, their voltage stress is lower than in the S-S compensation. Moreover, since the components L_{f1}, C_{f1} resonate at the nominal operating frequency, the inverter's current high-order harmonic components are highly attenuated. This ensures low distortion of I_1 that is fundamental to fulfill the electromagnetic compatibility (EMC) limits for the radiated magnetic field [17].

First, it is verified the suitability of the S-S compensation network with the given coils. This is done by checking if it satisfies all the requirements in Table I. If not, the double-sided LCC compensation would be selected and designed.

A. S-S compensation network

The resulting circuit's parameters of the S-S compensation network are shown in Table II. By using (1) and (2), the S-S compensation network satisfies the output requirements on P_{out} and V_{out} specified in Table I. According to [5]–[10], the compensation capacitance of both the primary and secondary circuits are calculated as: $C_1 = \frac{1}{\omega_0^2 L_1}, C_2 = \frac{1}{\omega_0^2 L_2}$. In both circuits, the components' voltages and currents can be computed with the Kirchhoff's voltage law in (3) and (4). These equations use the phasor convention, where all voltages and currents are assumed to be 85 kHz sinusoids, and $\boldsymbol{V}_{AB}$ is taken as reference such that $\boldsymbol{V}_{AB} = V_{AB}\underline{/0°}$. The DC input voltage V_{in} can be found by using (5). Both (2) and (5) are based on the first harmonic approximation (FHA) [11], [18].

$$I_{out} = \frac{P_{out}}{V_{out}} \tag{1}$$

$$I_2 = \frac{\pi}{\sqrt{2} \cdot 2} I_{out} \tag{2}$$

$$\boldsymbol{V}_{AB} = (R_1 + j\omega L_1 + \frac{1}{j\omega C_1})\boldsymbol{I}_1 + j\omega M \boldsymbol{I}_2 \tag{3}$$

$$0 = (R_2 + R_{ac} + j\omega L_2 + \frac{1}{j\omega C_2})\boldsymbol{I}_2 + j\omega M \boldsymbol{I}_1 \tag{4}$$

$$V_{in} = \frac{\pi}{4} V_{AB} \tag{5}$$

To verify if the S-S compensation is suitable, the results of Table II must be compared to the requirements in Table I. It is possible to notice that the resulting DC input voltage V_{in} is not within any of the allowed ranges. There are two possible ways to overcome this issue. V_{in} could be stepped up by inserting a highly-coupled transformer between the compensation capacitor C_1 and the coil L_1, with a turns ratio greater

V_{in}	112.3 V
C_1, C_2	55.34 nF, 80.5 nF
$\hat{I}_1$, $\hat{I}_2$	129.7 A, 30.2 A
$\hat{V}_{L1}$, $\hat{V}_{L2}$	4.4 kV, 703 V
$\hat{V}_{C1}$, $\hat{V}_{C2}$	4.4 kV, 703 V

Fig. 3.   Simulated V_{AB} and $I_{L_{f1}}$ at: a) $V_{in} = 380\,\text{V}$, b) $V_{in} = 650\,\text{V}$.

than the unity. However, this solution is not ideal because the losses in the transformer would be considerable due to the high-frequency operation. Another possibility would be to add a DC/DC converter in either the primary or secondary side. However, this would increase the cost and reduce the total efficiency. Additionally, with any of these solutions, the requirements on $\hat{I}_1$ would not be satisfied because it exceeds the maximum rated value for the primary coil.

It can be concluded that the S-S compensation network is not preferable in this application. This means that the double-sided LCC compensation network should be investigated.

B. Double-sided LCC compensation network

The circuit parameters' definition and detailed analysis of the double-sided LCC compensation can be found in [12]. The parameters' definition is summarized in (6). However, in [12], the value of the parameters is chosen only for a completely symmetrical system, and not for a generalized approach.

$$L_{fi}C_{fi} = \frac{1}{\omega_0^2}, \quad L_i - L_{fi} = \frac{1}{\omega_0^2 C_i} \qquad i = 1, 2 \quad (6)$$

The values of L_1, L_2, and M are known, which are listed in Table I. The values of L_{f1}, L_{f2} need to be selected according to the requirements on P_{out} and V_{out}. After this, the values of C_1, C_2, C_{f1} and C_{f2} can be computed as shown in (6).

The double-sided LCC compensation has a constant-current output characteristic, since $\hat{I}_{L_{f2}}$ is load-independent [12]:

$$\hat{I}_{L_{f2}} = \frac{M\frac{4}{\pi}V_{in}}{\omega_0 L_{f1}L_{f2}} \quad (7)$$

To make sure that the double-sided LCC meets the output requirements, the relation between $\hat{I}_{L_{f2}}$ and I_{out} is described by (8). This is based on [18] that assumes a continuous conduction of the rectifier's diodes in Fig. 1a).

$$\hat{I}_{L_{f2}} = \frac{\pi}{2}I_{out} \quad (8)$$

By substituting (7) and (1) into (8), it can be found that

$$L_{f1}L_{f2} = \frac{8}{\pi^2}\frac{MV_{in}V_{out}}{\omega_0 P_{out}} \quad (9)$$

In (9), there are two unknown variables: the ratio between L_{f1} and L_{f2}, and the input voltage V_{in}. The ratio between L_{f1} and L_{f2} can be found by choosing the desired amount of coils' current. In this case, the coils are chosen to carry the same amount of current to keep the components' voltage and current stress under control. Since [12] defines $\hat{I}_1$ and $\hat{I}_2$ as in (10), the condition that makes $\hat{I}_1 = \hat{I}_2$ is (11). At this
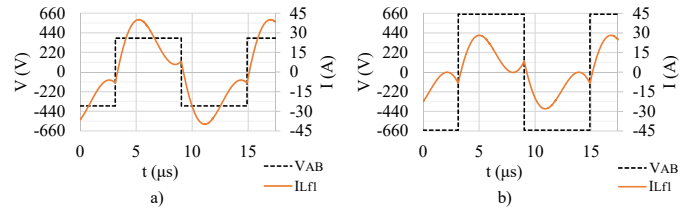
point, L_{f1} and L_{f2} can be calculated by using (9) and (11). However, before that, the proper V_{in} needs to be selected.

$$\hat{I}_1 = \frac{\frac{4}{\pi}V_{in}}{\omega_0 L_{f1}}, \qquad \hat{I}_2 = \frac{\frac{4}{\pi}V_{out}}{\omega_0 L_{f2}} \quad (10)$$

$$\frac{L_{f2}}{L_{f1}} = \frac{V_{out}}{V_{in}} \quad (11)$$

According to (9), it can be found that V_{out} is directly proportional to both M and V_{in}. This means that, when the coils become more misaligned, the target P_{out} can be reached by increasing V_{in}. Therefore, at the highest coupling condition, the compensation network has to be tuned at the minimum V_{in}. Table I shows two possible ranges of V_{in} depending on the grid connection. Herein, it is assumed an operation at $V_{in} = 380\,\text{V}$ for the 1ϕ grid connection, while $V_{in} = 650\,\text{V}$ for the 3ϕ grid connection. To identify which grid connection is the most suitable, a double-sided LCC compensation network is designed for both minimum values of V_{in} based on (6), (9) and (11). Circuit simulations in the time domain show that $I_{L_{f1}}$ and $I_{L_{f2}}$ are distorted. This happens because the LCC components have multiple frequencies that influence the resonance at 85 kHz. This means that (9) and (11) are not accurate since they are based on the FHA. Therefore, to reach $P_{out} = 7.7\,\text{kW}$, a higher value of P_{out} has been used in (9).

To make a fair comparison, both solutions are designed to have soft-switching operation. As explained in [12], [18]–[21], the zero-voltage switching (ZVS) turn-on can be realized by switching off the inverter legs at a turn-off current I_{OFF} that is high enough to completely discharge the equivalent drain-source internal capacitance C_{ds} of the MOSFETs during the dead time t_{dead}. To perform the comparison, the two designs are tuned to the same I_{OFF} as it is shown in Fig. 3. By using (6), (9) and (11), the design at $V_{in} = 650\,\text{V}$ reaches the operating condition shown in Fig. 3b). On the other hand, at $V_{in} = 380\,\text{V}$, to realize the same I_{OFF}, the capacitance C_2 has been increased by 6.1 nF as explained in [12]. Since the value of I_{OFF} depends on $V_{ds,off}$, C_{ds} and t_{dead}, I_{OFF} varies for different MOSFETs and V_{in}. Hereby, this is not considered because it is out of the scope of the paper.

The components used for both the inverter and the compensation network are listed in Table III. For both possible V_{in}, two SiC MOSFETs are considered that differ in current rating and, consequently, in price. The resulting circuit's parameters for both designs of the double-sided compensation network are shown in Table IV, where the number and type of passive components are specified within the brackets. The two designs are analyzed for what concerns the components' voltage $\hat{V}$ and

TABLE III
COMPONENTS USED FOR THE INVERTER AND COMPENSATION NETWORK.

	Comp.	Manufacturer + n.	Cost ($)	R_s (Ω)
SiC	SW1	Cree/Wolfspeed C3M0120090D	6.025[1]	0.156[4]
	SW2	Cree/Wolfspeed C3M0065090D	9.375[1]	0.083[4]
	SW3	Cree/Wolfspeed C2M0160120D	7.812[1]	0.264[4]
	SW4	Cree/Wolfspeed C3M0075120K	11.875[1]	0.094[4]
LCC	6.8 nF	EPCOS B32671L0682J000	0.160[2]	0.100[5]
	3.3 µH	Würth Elektronik 7443640470	6.832[3]	0.073[5]
	4.7 µH	Würth Elektronik 74436410330	6.832[3]	0.090[5]

N. of units: [1]500+, [2]5000+, [3]270+, from Digi-key [22]. [4]Datasheet @125 °C, [5]Measured @85 kHz.

TABLE IV
PARAMETERS OF THE DOUBLE-SIDED LCC COMPENSATION NETWORK FOR BOTH POSSIBLE V_{in}.

V_{in}	380 V (1φ)	650 V (3φ)
L_{f1}	14.17 µH (4.7 · 3)µH	23.54 µH (3.3 · 3 + 4.7 · 3)µH
L_{f2}	14.91 µH (same as in 3φ)	14.49 µH (3.3 · 3 + 4.7 · 1)µH
C_{f1}	247.50 nF (6.8 nF · 2 × 72)	148.93 nF (6.8 nF · 2 × 44)
C_{f2}	235.13 nF (6.8 nF · 2 × 70)	242.02 nF (6.8 nF · 2 × 72)
C_1	71.28 nF (6.8 nF · 4 × 42)	88.07 nF (6.8 nF · 4 × 52)
C_2	128.60 nF (6.8 nF · 3 × 57)	120.70 nF (6.8 nF · 3 × 53)

TABLE V
POWER LOSS P_{loss} AND COST OF THE COMPENSATION AND INVERTER.

V_{in}	380 V		650 V	
	P_{loss} (W)	Cost ($)	P_{loss} (W)	Cost ($)
Coils	508.8	-	539.0	-
LCC	400.2	147.48	364.1	164.14
$\Sigma_{L,C}$	909.0	147.48	903.1	164.14
SiC	SW1/SW2 100.2/53.3	SW1/SW2 48.20/75.00	SW3/SW4 71.7/25.5	SW3/SW4 62.5/95.0
Total	1009.2/962.3	195.68/222.48	974.8/928.6	226.64/259.14

current $\hat{I}$ stress, conduction power losses P_{loss} and total cost. Table V shows the total P_{loss} and cost of all designs, where the partial quantities of the main coils, compensation network and inverter are highlighted. The cost of the main coils is not considered here, because it is the same for all designs and it is not interesting for the comparison. Additionally, the details of each passive component are shown in Table VI. At $V_{in} = 650$ V, the current stress on the inverter $\hat{I}_{L_{f1}}$ is about 30% lower than in the case of $V_{in} = 380$ V. On the other hand, at $V_{in} = 380$ V, the current stress on both the main coils $\hat{I}_1$, $\hat{I}_2$ is about 3% lower which leads to lower P_{loss} than in the case of $V_{in} = 650$ V. From Table V, it can be concluded that the total P_{loss} on the passive components $\Sigma_{L,C}$ is slightly lower (0.65%) for the 3φ grid connection ($V_{in} = 650$ V) at a cost that is 11% higher. Considering also the P_{loss} of the inverter, the case of $V_{in} = 380$ V with SW4 leads to the lowest total losses and most expensive design. To evaluate if the extra cost can be amortized with the time, the economical analysis of all the designs is performed in Table VII. The payback time is calculated taking as a reference the most affordable design ($V_{in} = 380$ V with SW1). As a result, the payback time of the most expensive and efficient solution with $V_{in} = 650$ V and SW4 is less than one year, which is much lower than the design lifetime of the wireless charging system. In a future work, this analysis will be verified experimentally with a prototype, where the primary circuitry is shown in Fig. 4.

IV. CONCLUSION

This paper explains the design and optimization of the compensation networks for a 7.7 kW wireless charging system which uses standardized coils of the power class WPT2. The conclusions can be summarized as follows:

TABLE VI
VOLTAGE $\hat{V}$ AND CURRENT $\hat{I}$ STRESS, POWER LOSS P_{loss} AND COST OF THE CIRCUIT PARAMETERS IN TABLE IV, FOR BOTH POSSIBLE V_{in}.

V_{in}		380 V	650 V		380 V	650 V
L_f	$\hat{I}$ (A)	39.9	28.2		39.1	39.4
	$\hat{V}$ (V)	896	896		619	607
	P_{loss} (W)	173.1	133.5		178.2	179.4
	Cost ($)	20.50	41.00		27.30	27.30
C_f	$\hat{I}$ (A)	82.8	77.2		84.7	86.4
	$\hat{V}$ (V)	609	990		669	665
	P_{loss} (W)	8.8	13.5		9.8	10.0
	Cost ($)	23.04	14.08		22.40	23.04
L	$\hat{I}$ (A)	63.7	65.4		63.4	65.2
	$\hat{V}$ (V)	2257	2375		1582	1664
	P_{loss} (W)	382.7	405.5		126.1	133.5
	Cost ($)	[3]	[3]		[4]	[4]
C	$\hat{V}$ (V)	1683	1402		933	1020
	P_{loss} (W)	19.5	16.7		10.7	12.2
	Cost ($)	26.88	33.28		27.36	25.44

(Left pair of columns: **primary**; right pair of columns: **secondary**.)

TABLE VII
ECONOMICAL EVALUATION BASED ON THE DAILY POWER CONSUMPTION.

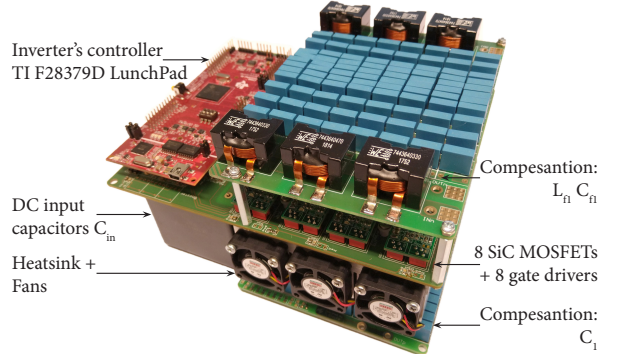| V_{in}		$P_{in}^{[1]}$	E_{in}/day[2]	Cost/day[3]	Payback t[4]
380 V	SW1	8.71 kW	70.1 kWh	16.13$	0 years
	SW2	8.66 kW	69.7 kWh	16.04$	0.84 years
650 V	SW3	8.67 kW	69.8 kWh	16.06$	1.31 years
	SW4	8.63 kW	69.46 kWh	15.98$	0.67 years

[1] $P_{in} = P_{out} + P_{loss(total)}$ according to Table I and V.
[2] One EV with a battery of 62 kWh is fully charged per day.
[3] Calculated with the 2019 electricity price (0.23$/kWh) of the Netherlands.
[4] Payback $t = \dfrac{Cost_{LCC+SWn} - Cost_{LCC+SW1}}{365 \cdot (Cost/day_{SW1} - Cost/day_{SWn})}$, where $n = 1 \dots 4$.

Fig. 4. Primary-side prototype to be used with the coils in Fig. 2.

(Labels in figure: Inverter's controller TI F28379D LunchPad; DC input capacitors C_{in}; Heatsink + Fans; Compensation: L_{f1} C_{f1}; 8 SiC MOSFETs + 8 gate drivers; Compensation: C_1)

– The series-series compensation network is proved to be unfeasible with the selected coils because, to match the output requirements, it demands a DC input voltage that is below the minimum value allowed by any grid connection. It also causes a high current stress at the primary circuit which is higher than the coil's rated value.

– The double-sided LCC compensation network is found to be more suitable for this application. The 3-phase grid connection is selected, because the DC input voltage range 650-870 V ensures soft-switching of the inverter at 85 kHz, low current stress on the inverter and the lowest total conduction losses on the passive components.

– Two parallel 1200V SiC MOSFETs C3M0075120K are chosen as switch of the inverter because of their low conduction losses. Taking as a reference the cheapest design, this solution has a payback time less than one.

References

[1] F. Grazian, W. Shi, J. Dong, P. van Duijsen, T. B. Soeiro, and P. Bauer, "Survey on standards and regulations for wireless charging of electric vehicles," in *AEIT International Conference of Electrical and Electronic Technologies for Automotive (AEIT AUTOMOTIVE)*, 2019.

[2] *J2954 RP: Wireless Power Transfer for Light-Duty Plug-In/ Electric Vehicles and Alignment Methodology*, SAE International Std., Apr. 2019.

[3] MAGMENT. Magnetic concretes. Accessed: 07/11/2019. [Online]. Available: https://www.magment.de/en-products

[4] PREMO. Wc-rx-002-90k receiving antenna exible-pad for the wireless power transfer in the electric vehicles. Accessed: 07/11/2019. [Online]. Available: https://www.grupopremo.com/689-wc-rx-002-90k-receiving-antenna-flexible-pad-for-the-wireless-power-transfer-in-the-electric-vehicles

[5] C.-S. Wang, G. Covic, and O. Stielau, "General stability criterions for zero phase angle controlled loosely coupled inductive power transfer systems," in *27th Annual Conference of the IEEE Industrial Electronics Society (IECON)*, 2001.

[6] C. S. Wang, G. Covic, and O. Stielau, "Power transfer capability and bifurcation phenomena of loosely coupled inductive power transfer systems," *IEEE Transactions on Industrial Electronics*, vol. 51, pp. 148 – 157, 2004.

[7] C.-S. Wang, O. Stielau, and G. Covic, "Design considerations for a contactless electric vehicle battery charger," *IEEE Transactions on Industrial Electronics*, vol. 52, pp. 1308 – 1314, 2005.

[8] S. Chopra and P. Bauer, "Analysis and design considerations for a contactless power transfer system," in *IEEE 33rd International Telecommunications Energy Conference (INTELEC)*, 2011.

[9] S. Li and C. C. Mi, "Wireless power transfer for electric vehicle applications," *IEEE Journal of Emerging and Selected Topics in Power Electronics*, vol. 3, pp. 4 – 17, 2015.

[10] Z. Zhang, H. Pang, A. Georgiadis, and C. Cecat, "Wireless power transferan overview," *IEEE Transactions on Industrial Electronics*, vol. 66, pp. 1044 – 1058, 2019.

[11] S.-Y. Cho, I.-O. Lee, S. Moon, G.-W. Moon, B.-C. Kim, and K. Y. Kim, "Series-series compensated wireless power transfer at two different resonant frequencies," in *IEEE ECCE Asia Downunder*, 2013.

[12] S. Li, W. Li, J. Deng, T. D. Nguyen, and C. C. Mi, "A double-sided lcc compensation network and its tuning method for wireless power transfer," *IEEE Transactions on Vehicular Technology*, vol. 64, pp. 2261 – 2273, 2015.

[13] W. Li, H. Zhao, J. Deng, S. Li, and C. C. Mi, "Comparison study on ss and double-sided lcc compensation topologies for ev/phev wireless chargers," *IEEE Transactions on Vehicular Technology*, vol. 65, pp. 4429 – 4439, 2016.

[14] Q. Zhu, L. Wang, Y. Guo, C. Liao, and F. Li, "Applying lcc compensation network to dynamic wireless ev charging system," *IEEE Transactions on Industrial Electronics*, vol. 63, pp. 6557 – 6567, 2016.

[15] V.-B. Vu, D.-H. Tran, and W. Choi, "Implementation of the constant current and constant voltage charge of inductive power transfer systems with the double-sidedlcccompensation topology for electric vehicle battery charge applications," *IEEE Transactions on Power Electronics*, vol. 33, pp. 7398 – 7410, 2018.

[16] Y. Zhang, Z. Yan, T. Kan, Y. Liu, and C. C. Mi, "Modelling and analysis of the distortion of strongly-coupled wireless power transfer systems with ss and lcclcc compensations," *IET Power Electronics*, vol. 12, pp. 1321 – 1328, 2019.

[17] W. Shi, F. Grazian, J. Dong, , T. B. Soeiro, and P. Bauer, "Analysis of magnetic field emissions in inductive power transfer ev chargers following reference designs in sae j2954/2019," in *IEEE International Symposium on Circuits and Systems (ISCAS)*, 2020.

[18] R. Steigerwald, "A comparison of half-bridge resonant converter topologies," *IEEE Transactions on Power Electronics*, vol. 3, pp. 174 – 182, 1988.

[19] B. Lu, W. Liu, Y. Liang, F. Lee, and J. van Wyk, "Optimal design methodology for llc resonant converter," in *Twenty-First Annual IEEE Applied Power Electronics Conference and Exposition (APEC)*, 2006.

[20] T. Kan, T.-D. Nguyen, J. C. White, R. K. Malhan, and C. C. Mi, "A new integration method for an electric vehicle wireless charging system using lcc compensation topology: Analysis and design," *IEEE Transactions on Power Electronics*, vol. 32, pp. 1638 – 1650, 2017.

[21] F. Grazian, P. van Duijsen, T. B. Soeiro, and P. Bauer, "Advantages and tuning of zero voltage switching in a wireless power transfer system," in *IEEE PELS Workshop on Emerging Technologies: Wireless Power (WoW)*, 2019.

[22] "Digi-key electronics." [Online]. Available: https://www.digikey.com/